

CONTROL OF LASER RADIATION PARAMETERS

PACS numbers: 42.55.Wd, 42.55.Ye, 42.65.Dr; 42.60.Da
DOI: 10.1070/QE2003v033n12ABEH002560

Dependence of the spectral parameters of a Raman fibre laser on the Bragg grating temperature

S.A. Babin, A.S. Kurkov, V.V. Potapov, D.V. Churkin

Abstract. **Changes in the output power and emission spectrum of a two-stage Raman phosphosilicate fibre laser are measured during the temperature tuning of fibre Bragg gratings (FBGs) forming enclosed resonators (1.26/1.52 μm). The output emission spectrum of the dense resonator (1.26 μm) is split into two components, whose relative amplitudes change during the temperature tuning of FBGs. A simple analytic model is constructed which describes the broadening and splitting of the spectrum as well as the appearance of its asymmetry upon the relative detuning of FBGs. It is shown that these effects result in the increase in the effective transmission coefficient of the dense resonator at least by an order of magnitude, which affects the output power of the Raman laser.**

Keywords*: fibre laser, Raman converter, fibre Bragg grating, gain saturation.*

1. Introduction

Currently Raman fibre amplifiers operating at wavelengths of 1.3 and 1.5 μm and Raman germanosilicate [1, 2] and phosphosilicate [3 – 6] fibre lasers for their pump have been actively developed and studied. These devices play a very important role in modern communication systems; however, the physical mechanisms of their operation have not been adequately investigated.

The operation of single-, two-, and multistage Raman lasers of different designs was numerically simulated in Refs [7 – 9]. The aim of these studies was to obtain the optimal parameters (the resonator length, the transmission coefficient of the input mirror) providing the maximum output power and maximum conversion efficiency. In particular, the longitudinal distribution of the pump power and generated Stokes components in the resonator was calculated. Assuming that the power is independent of the coordinate along the resonator, an analytic expression was obtained for the efficiency at each stage of the radiation conversion [7], a linear increase in the output power of the converter with increasing pump power was explained and experimental setups were optimised according to numerical calculations [8, 9].

In this paper, we analysed the spectral parameters of the Stokes components in a Raman fibre laser and their changes upon tuning the working wavelength of FBGs forming the resonator, which is important for understanding the physical mechanisms of lasing and optimisation of the laser parameters.

2. Experiment

Figure 1 shows the scheme of the experimental setup. An ytterbium-doped fibre laser was pumped by a 0.98-μm, 8-W Milon-500 diode laser. The efficiency of the 0.98-μm multimode radiation conversion from the diode laser to the 1.08-μm single-mode radiation of the ytterbium-doped laser was 56 %. A Raman phosphosilicate fibre converter was spliced to the output of the ytterbium-doped fibre laser. The large Stokes shift of the converter (~ 1330 cm^{-1}) made it possible to obtain lasing in the region of ~ 1.5 micron by the two-stage conversion of radiation from the ytterbium-doped fibre laser.

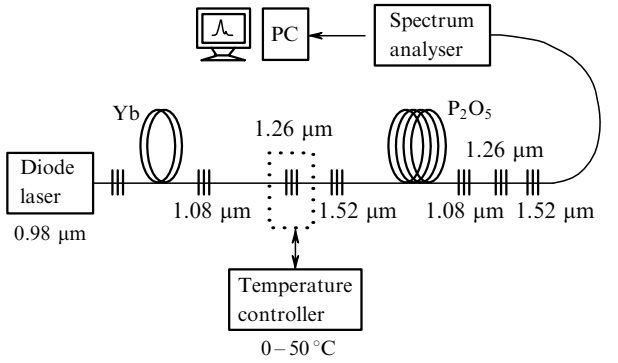

Figure 1. Scheme of the experimental setup.

Two enclosed resonators formed by FBGs reflecting at 1.26 and 1.52 μm provided the radiation conversion according to the $1.08 \rightarrow 1.26 \rightarrow 1.52$ μm scheme. The reflectivity of all gratings exceeded 99 % except the reflectivity of the output grating, which was 42 % (2.3 dB) at a wavelength of 1.52 μm. To provide stronger absorption of radiation from the ytterbium-doped fibre laser, an additional grating with

S.A. Babin, V.V. Potapov, D.V. Churkin Institute of Automation and Electrometry, Siberian Branch, Russian Academy of Sciences, prosp. Koptyuga 1, 630090 Novosibirsk, Russia;
A.S. Kurkov Fiber Optics Research Center, A.M. Prokhorov General Physics Institute, Russian Academy of Sciences, ul. Vavilova 38, 119991 Moscow, Russia

Received 20 March 2003
Kvantovaya Elektronika **33** (12) 1096 – 1100 (2003)
Translated by M.N. Sapozhnikov

the reflectivity $\sim 100\,\%$ at 1.08 μm was placed in the output stage of the gratings. This way, two-pass pump was realised.

The dependence of the output power of the converter on the pump power (Fig. 2) can be divided into three characteristic regions. In the first region, when the pump power $P_{0.98} < 0.75$ W, no Stokes frequency conversion occurs, and the transmitted pump radiation at $\lambda_0 = 1.08$ μm of power no more than 1 mW is detected at the output. Above the threshold for the first Stokes component ($P_{0.98} \geqslant 0.75$ W), lasing appears at 1.26 μm. The conversion efficiency $P_{1.26}/P_{0.98}$ of this process is $\sim 8\,\%$. In the third region ($P_{0.98} > 2.5$ W), the second Stokes component at 1.52 μm becomes involved in lasing, and the converter efficiency increases up to $\sim 17\,\%$.

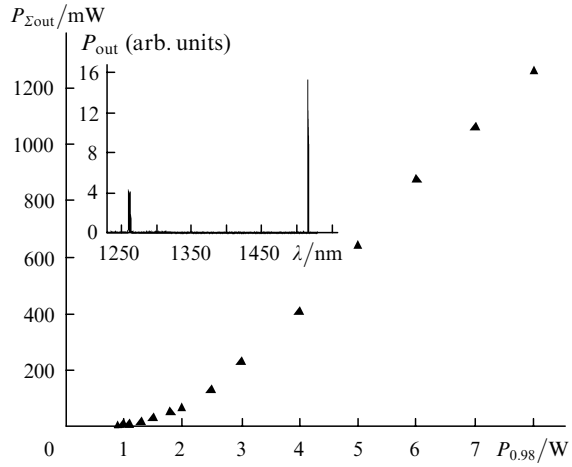

Figure 2. Dependence of the total output power $P_{1.52} + P_{1.26}$ on the diode pump power $P_{0.98}$. The inset shows the spectrum of the converter for $P_{0.98} = 4$ W.

The typical emission spectrum of the Raman laser is shown in the inset in Fig. 2. The spectrum exhibits a narrow peak at 1.52 μm of width $\Delta\lambda \lesssim 0.4$ nm at the diode pump power $P_{0.98} = 4$ W; the peak width increases up to 0.75 nm at $P_{0.98} = 8$ W. The output emission spectrum of the dense resonator at 1.26 μm is split into two components, which was observed earlier (see, for example, Ref. [4]). The central wavelengths are determined by the maximum reflection wavelengths of FBGs. The working wavelength of a FBG can be changed by increasing (decreasing) the grating temperature or by stretching (compressing) the grating.

We tuned FBGs using thermoelectric elements. When the temperature of the output grating was changed within $\pm 0.25\,^{\circ}$C (corresponding to the wavelength change $\Delta\lambda \simeq \pm 0.25$ nm), the symmetric output emission spectrum (Fig. 3a) became asymmetric (Figs 3b, c). As the temperature of the input grating was decreased, the emission spectrum was distorted as upon increasing the output grating temperature. In this case, the total output power of the converter changed insignificantly, and the power at 1.52 μm change approximately by $15\,\% - 20\,\%$ (Figs 4b, c). The greatest changes occur near the lasing threshold, when, using the temperature tuning of the gratings, the lasing threshold can be decreased (increased) or lasing can be produced (quenched) at a given pump power (Fig. 4a). Note that upon the red shift of the reflection spectrum of the input grating during its heating, the output power maximum, as expected, also shifts to the red, whereas upon the shift of the reflection spectrum of the output grating to the red, the output power maximum shifts, on the contrary, to the blue. The temperature tuning of the resonator grating reflecting at 1.52 μm does not cause any noticeable changes in the shape of the emission spectrum of the Raman laser, the spectrum being only slightly shifted. Note that the characteristic shape of the spectrum at 1.26 μm (splitting and asymmetry caused by the detuning of gratings) was observed both at diode pump powers $P_{0.98} < 2.3$ W providing lasing only at 1.26 μm and at higher pump powers ($P_{0.98} > 2.3$ W), when lasing was also observed at 1.52 μm.

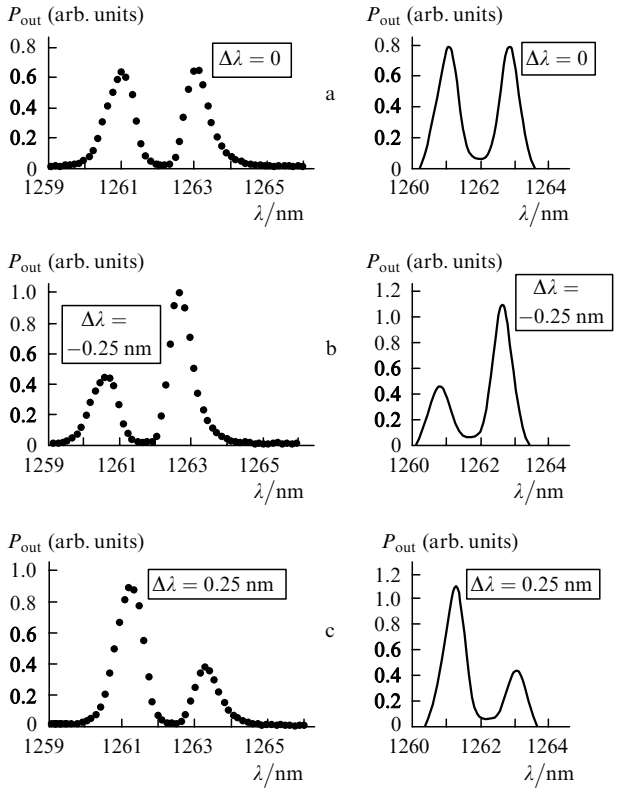

Figure 3. Experimental (left) and calculated (right) output emission spectra at 1.26 μm for different detunings of the output grating of the first stage.

3. The model

To explain the splitting and asymmetry of the output emission spectrum of a dense resonator in the intermediate stage, we consider the lasing model for a single-stage Raman fibre laser. According to Refs [7, 10, 11], we write the system of equations

$$\frac{\mathrm{d}P_0^{\pm}}{\mathrm{d}z} = \mp\left[k_0 g_0 \left(P_1^{+} + P_1^{-}\right) P_0^{\pm} + \alpha_0 P_0^{\pm}\right],$$
$$\frac{\mathrm{d}P_1^{\pm}}{\mathrm{d}z} = \pm\left[g_0 \left(P_0^{+} + P_0^{-}\right) P_1^{\pm} - \alpha_1 P_1^{\pm}\right], \qquad (1)$$

where $P_0^{\pm}$ and $P_1^{\pm}$ are the powers of the pump and Stokes waves, respectively, propagating in the positive (+) and negative (−) directions of the z axis; $k_0 = \lambda_1/\lambda_0$ is the ratio

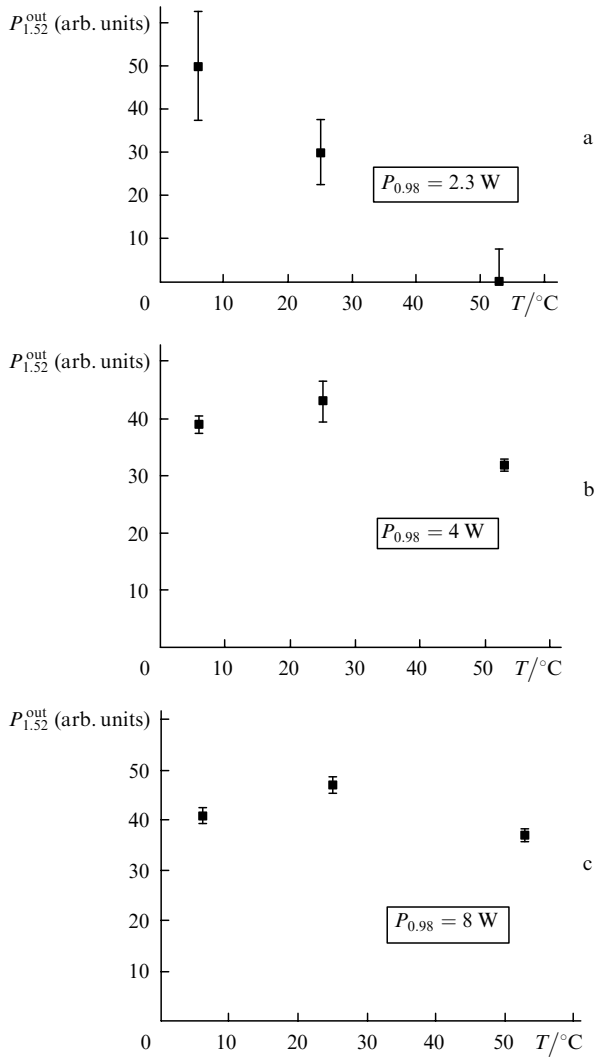

Figure 4. Dependences of the output power $P_{1.52}^{out}$ on the grating temperature T for different diode pump powers $P_{0.98}$.

of the Stokes component and pump wavelengths; α_i is the absorption coefficient; and g_0 is the Raman gain in the fibre.

The system of equations (1) should be supplemented with the boundary conditions: the pump power P_0^{in} of the Raman laser and the conditions of the radiation reflection from FBGs. Assuming that the pump radiation is completely reflected from the input grating at 1.08 μm, we obtain

$$\begin{aligned} P_1^-(l,\lambda) &= R_2(\lambda)P_1^+(l,\lambda), \\ P_1^+(0,\lambda) &= R_1(\lambda)P_1^-(0,\lambda), \\ P_0^+(l) &= P_0^-(l), \\ P_0^{in} &= P_0^+(0) + P_0^-(0). \end{aligned} \tag{2}$$

Here, $R_1(\lambda)$ and $R_2(\lambda)$ are the spectral profiles of the input and output gratings and l is the resonator length.

The numerical calculations performed in Ref. [7] show that the value of $2P_1 = (P_1^+ + P_1^-)$ weakly depends on z. Then, assuming that $P_1 = \text{const}$, we integrate the system (1) at the specified boundary conditions (2). The required intracavity power $P_1(\lambda)$ is the solution of the transcendental equation

$$[2k_0g_0P_1 + \alpha_0][\alpha_1 l - \frac{1}{2}\ln(R_1R_2)] = g_0P_0^{in}\tanh[(2k_0g_0P_1 + \alpha_0)l]. \tag{3}$$

Even when the pump power only slightly exceeds the Stokes component lasing threshold, the value of $(2k_0g_0P_1 + \alpha_0)l$ is large, so that $\tanh[2k_0g_0P_1 + \alpha_0)l] \approx 1$, and the intracavity power is described by the expression

$$P_1 = \frac{P_0^{in}/(2k_0)}{\alpha_1 l - (1/2)\ln(R_1R_2)} - \frac{\alpha_0}{2k_0g_0}. \tag{4}$$

In this case, as for a conventional laser, we can introduce the saturated gain g for the Stokes wave

$$g(P_1) = g_0\left(1 + \frac{2k_0g_0}{\alpha_0}P_1\right)^{-1}. \tag{5}$$

Then, expression (4) follows from the condition of the equality of the gain and losses after the round trip of radiation in the resonator with the average pump power $\bar{P}_0 = P_0^{in}/(2\alpha_2 l)$. Note that the saturation of the gain for the Stokes wave with increasing its power P_1 is caused by the pump depletion ($P_0^{out} < P_0^{in}$). Assuming that the Raman line is broadened inhomogeneously and lasing at modes with different wavelengths occurs independently, we can obtain the spectral dependence of the power $P_1(\lambda)$, knowing the spectral dependences of the reflection coefficients $R_1(\lambda)$ and $R_2(\lambda)$ of the input and output FBGs. The output power P_{out} is a product of the intracavity power P_1 by the transmission coefficient $(1 - R_2)$ of the output grating

$$P_{out}(\lambda) = P_1(\lambda)[1 - R_2(\lambda)]. \tag{6}$$

The spectral characteristic $R_i(\lambda)$ of the gratings was determined by approximating the experimental transmission spectrum of the grating (Fig. 5). The typical width of the Raman gain line is ~ 10 nm [8], so that g_0 can be assumed constant at the scale $\Delta\lambda \sim 1$ nm. A phosphosilicate fibre used in experiments had the following optical losses and Raman gains: $\alpha_0 = 1.8$ dB km^{-1}, $\alpha_1 = 0.92$ dB km^{-1}, $\alpha_2 = 1$ dB km^{-1}; $g_0 = 5.6$ dB km^{-1} W^{-1} and $g_1 = 4.1$ dB km^{-1} W^{-1}. The output emission spectra calculated from expression (4) are presented in Figs 3a–c for the corresponding exper-

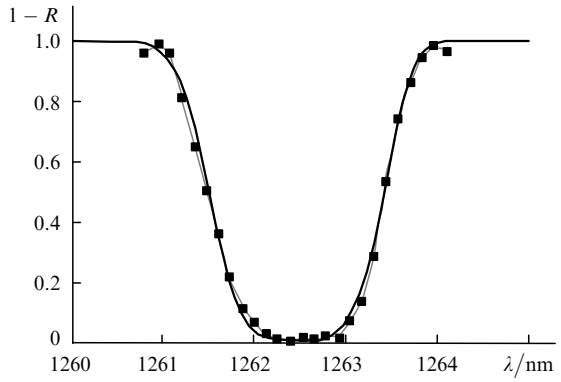

Figure 5. Transmission spectrum of the grating.

imental conditions. As in the experiment, when the spectrum of the output gratin shifted to the red, the maximum of lasing shifted in the opposite direction.

4. Discussion and conclusions

The obtained spectra can be simply qualitatively interpreted (Fig. 6). If the input and output gratings are centred at the same wavelength (Fig. 6a), then the profile of the intracavity power will be centred at this wavelength (Fig. 6b). In this case, the transmission coefficient of the output grating of the dense resonator is close to zero at the wavelengths where the intracavity power is maximal, and, hence, the output power will be very low. At the wavelengths where the transmission coefficient is close to unity, the intracavity power is close to zero, therefore, the output power at these wavelengths also will be very low.

The peaks in the output power spectrum are located between these two extreme positions and are determined by the optimal transmission coefficient of the output grating, which is achieved at two wavelengths that are symmetrical with respect to the central wavelength of the grating, i.e., the output emission spectrum is split (solid curve in Fig. 6).

When the temperature of the output grating changes, its spectrum shifts with respect to that of the input grating (Fig. 6a) (the output grating spectrum is shifted by $\Delta\lambda = 0.25$ nm to the red). In this case, the intracavity power spectrum (Fig. 6b) also shifts to the red, but to a lesser extent (half the above shift).

Therefore, because of the different spectral shifts of the intracavity power and the transmission coefficient of the output grating, the output emission spectrum becomes asymmetric (Fig. 6c). In this case, the red shift of the output grating spectrum results unexpectedly in the increase in the left peak because the optimal transmission for this peak is achieved at a high intracavity power, which was observed in the experiment. A different situation is observed when the input grating is tuned. In this case, the power maximum shifts in the same direction as the input grating spectrum. Note that, when the highly reflecting output mirror is replaced by a grating with the reflection coefficient

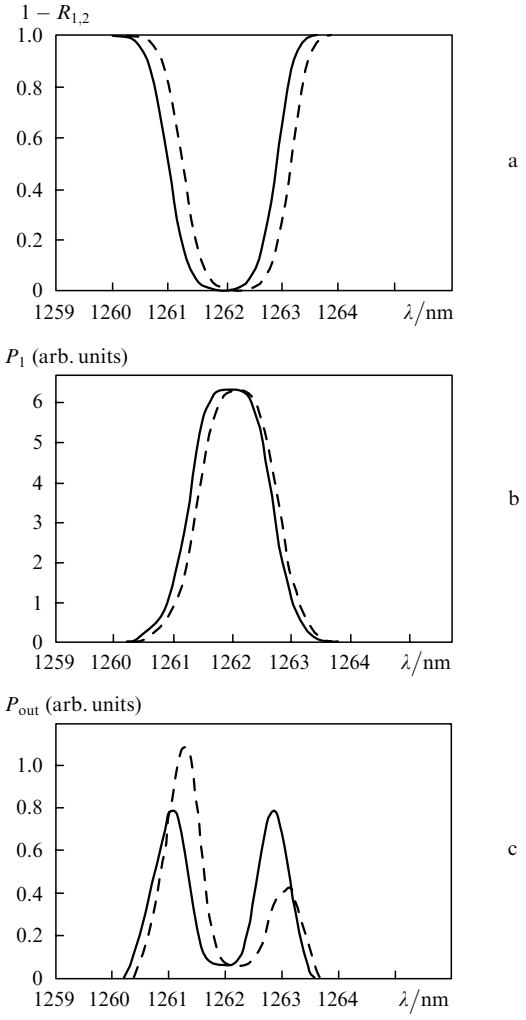

Figure 6. Transmission spectra $1 - R_{1,2}$ of the gratings (a), intracavity power P_1 (b) and output emission P_{out} (c) spectra calculated for $R_1^{max} = R_2^{max} = 99\,\%$. The solid curves correspond to the coinciding spectra of the input and output gratings ($\Delta\lambda = 0$); the dashed curves correspond to the shift of the output grating spectrum $R_2(\lambda)$ by 0.25 nm with respect to $R_1(\lambda)$.

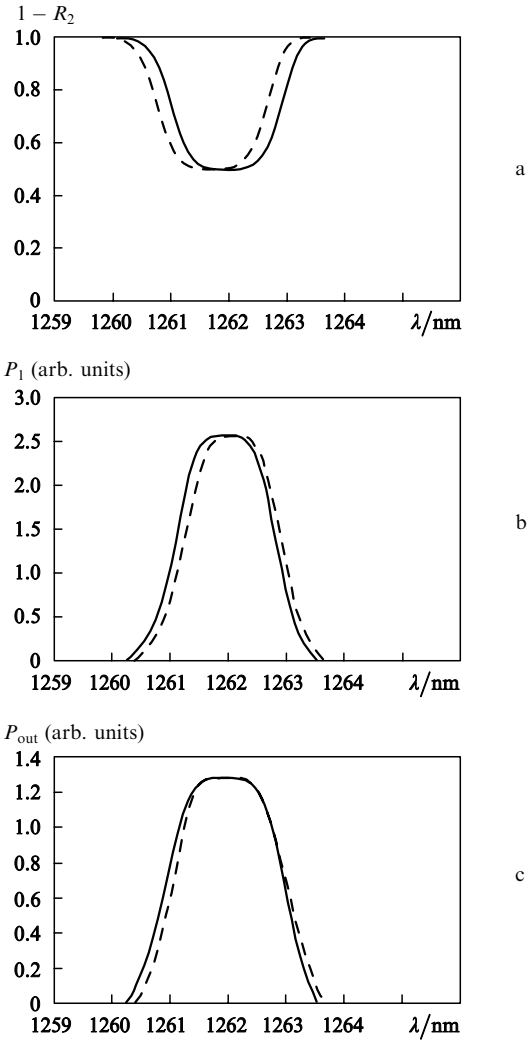

Figure 7. Transmission spectra $1 - R_2$ of the grating (a), intracavity power P_1 (b) and output emission P_{out} (c) spectra calculated for $R_1^{max} = 99\,\%$ and $R_2^{max} = 50\,\%$. The solid curves correspond to the coinciding spectra of the input and output gratings ($\lambda = 0$); the dashed curves correspond to the shift of the output grating spectrum $R_2(\lambda)$ by 0.25 nm with respect to $R_1(\lambda)$.

$\sim 50\,\%$, the splitting of the spectrum disappears (Fig. 7). The output power spectrum of the second Stokes component at 1.52 μm looks as shown in Fig. 7. In the case of a synchronous shift of the input and output gratings, the emission frequency is tuned without the change in the shape of the spectrum.

It is very important that well above the lasing threshold, the end effects make a substantial contribution to the converter parameters, and the integrated (over all λ) reflection coefficient of the grating strongly differs from the optimum coefficient. This effect is enhanced in the case of the relative spectral detuning of the gratings. According to our estimate, the effective transmission increases at least by an order of magnitude. This effect should influence the lasing threshold and power $P_{1.52}$ of the second Stokes component (Fig. 4).

Thus, we have studied experimentally the spectral characteristics of the two-stage fibre Raman converter by tuning the reflection spectra of FBGs forming the resonator. We have explained the splitting and asymmetry of the spectrum in a dense resonator and estimated a change in the effective transmission of the gratings caused by the end effects. Note that we used a rather crude model: because the saturation of the Raman gain in this model is determined by the pump depletion, lasing at different spectral components will not be independent. Other saturation mechanisms can be also involved, but the results will not change if the phenomenological expression of the type $g(P_1) \simeq g_0/(1+P_1/P_1^0)$ is valid, where $P_1^0(\alpha_0, g_0, l, \ldots)$ is the characteristic saturation intensity.

Acknowledgements. The authors thank E.V. Podivilov for useful discussions. This work was supported by a grant of the Siberian Branch, Russian Academy of Sciences.

References

1. Dianov E.M., Fursa D.G., Abramov A.A., Belovolov M.I., Bubnov M.M., Shipulin A.V., Prozorov A.M., Devyatykh G.G., Gur'yanov A.N., Khopin V.F. *Kvantovaya Elektron.*, **21**, 807 (1994) [*Quantum Electron.*, **24**, 749 (1994)].
2. Grubb S.G., Erdogan T., Mizrahi V., Strasser T., Cheung W.Y., Reed W.A., Lemaire P.J., Miller A.E., Kosinski S.G., Nykolak G., Beker P.C., Peckham D.W., in *Proc. Top. Meet. Opt. Ampl. Appl.* (USA, Breckenridge, 1994, PD-3).
3. Dianov E.M., Grekov M.V., Bufetov I.A., Vasiliev S.A., Medvedkov O.I., Plotnichenko V.G., Koltashev V.V., Belov A.V., Bubnov M.M., Semjonov S.L., Prokhorov A.M. *Electron. Lett.*, **33**, 1542 (1997).
4. Kartov V.I., Dianov E.M., Paramonov V.M., Medvedkov O.I., Bubnov M.M., Semyonov S.L., Protopopov V.N., Egorova O.N., Hopin V.F., Guryanov A.N., Bachynski M.P., Clements W.R.L. *Opt. Lett.*, **24**, 887 (1999).
5. Kim N.S., Prabhu M., Li C., Song J., Ueda K. *Opt. Commun.*, **176**, 219 (2000).
6. Kurkov A.S., Paramonov V.M., Egorova A.N., Medvedkov O.I., Dianov E.M., Zalevskii I.D., Goncharov S.E. *Kvantovaya Elektron.*, **32**, 747 (2002) [*Quantum Electron.*, **32**, 747 (2002)].
7. Bufetov I.A., Dianov E.M. *Kvantovaya Elektron.*, **30**, 873 (2000) [*Quantum Electron.*, **30**, 873 (2000)].
8. Kurukitkoson N., Sugahara H., Turitsyn S.K., Egorova O.N., Kurkov A.S., Paramonov V.M., Dianov E.M. *Electron. Lett.*, **37**, 1281 (2001).
9. Rini M., Cristiani I., Degiorgio V., Kurkov A.S., Paramonov V.M. *Opt. Commun.*, **203**, 139 (2002).
10. Auyeung H., Yariv A. *J. Opt. Soc. Am.*, **69**, 803 (1979).
11. Rini M., Cristiani I., Degiorgio V. *IEEE J. Quantum. Electron.*, **36**, 1117 (2000).